Fourier transform ion cyclotron resonance mass spectrometry and theoretical studies of gas phase S_N2 nucleophilic substitution reactions at sp^3-carbon atoms

Alan R. Katritzky,*[,a] Richard D. Burton,[a] Ming Qi,[a] Petia A. Shipkova,[a] Clifford H. Watson,[a] Zofia Dega-Szafran,‡[,a] John R. Eyler,*[,a] Mati Karelson,*[,b] Uko Maran[a,b] and Michael C. Zerner*[,a]

[a] *Department of Chemistry, Center for Heterocyclic Compounds and Quantum Theory Project, University of Florida, Gainesville, Florida 32611-7200, USA*
[b] *Department of Chemistry, University of Tartu, 2 Jakobi St., Tartu, EE 2400, Estonia*

Gas phase S_N2 intramolecular displacements are reported in which neutral nucleophiles displace neutral leaving groups within cationic substrates. In the intramolecular S_N2 reaction of *N*-(2-piperidinoethyl)-2,4,6-triphenylpyridinium cation (11), the cationic product 12 was detected directly. Intramolecular reactions of *N*-(ω-aminoalkyl)-5,6,8,9-tetrahydro-7-phenyldibenzo[*c*,*h*]acridinium salts 13a–c, *N*-(5-hydroxypentyl)-5,6,8,9-tetrahydro-7-phenyldibenzo[*c*,*h*]acridinium salt 14 and *N*-(ω-aminoalkyl)-2,4,6-triphenylpyridinium salts 20a,b afforded the corresponding protonated acridinium cation (15) or pyridinium cation (21) and, presumably, a neutral heterocycle. This interpretation is supported by isotopic labeling control experiments. No evidence has been obtained for any intermolecular gas phase S_N2 reaction with a pyridine as leaving group; theoretical calculations suggest an explanation for these experimental results.

Introduction

One of the most important reactions in organic chemistry is the replacement of a leaving group (X) attached to an aliphatic carbon atom (R) by a nucleophile (Nu) [reaction (1)]. There are

$$Nu + RX \longrightarrow NuR + X \qquad (1)$$

four main charge-type classes of such reactions: the substrate (RX) can be neutral or positively charged whereas the nucleophile (Nu) can be neutral or negatively charged.[1] Ingold recognized the fundamental distinction between a one-step bimolecular S_N2 reaction of Nu with RX and a two-step process with an initial unimolecular S_N1 scission of RX into R and X followed by combination of R with Nu.[2]

Most of the classical nucleophilic substitution mechanistic work in solution has been carried out with neutral substrates. For these, an S_N1 process $RX \rightarrow R^+ + X^-$ involves the creation of charge in the transition state, a process which is effectively inhibited in all but strongly polar solvents. Such solvents can also behave as nucleophiles; it is often difficult to disentangle whether such a solvent is simply a medium of relative permittivity sufficiently high to allow charge creation, or whether the solvent is behaving as a nucleophile. These conceptual difficulties are avoided for cationic substrates because the charge is then spread in an S_N1 transition state, rather than created [reaction (2)]. Thus S_N1-type reactions of cationic substrates

$$R^+X \longrightarrow R^+ + X \qquad (2)$$

are expected to, and do, occur in non-nucleophilic solvents of low relative permittivity. Extensive studies in one of our research groups[1,3] of the behavior of *N*-alkylpyridinium cations as substrates for nucleophilic substitution over the period of 1978–1990 shed much light on their detailed mechanisms, successfully demonstrating four different mechanisms (*i*) classical S_N1, (*ii*) Winstein S_N1, (*iii*) classical S_N2 and (*iv*) Sneen S_N2 routes. It was shown that these four mechanisms all remain distinct at borderlines with no merging.

Previous work in the gas phase

Most of the published gas-phase work on nucleophilic substitution reactions has been carried out with neutral substrates; more specifically it has often involved halide anions displacing a similar moiety in alkyl halides. On the basis of both experimental and theoretical work, Brauman and co-workers demonstrated[4] that such gas-phase S_N2 reactions proceed over a potential energy surface with double-minima separated by a barrier, and that the energy of the reactants is higher than that of this transition state. The two minima correspond to ion–dipole complexes that form as stable intermediates on either side of the transition state, *e.g.* $Cl^-(CH_3Br)$ and $(ClCH_3)Br^-$ in the case of the Cl^-/CH_3Br reaction. The formation and isolation of stable intermediates in the gas-phase substitution reactions and the activation of those intermediates to form products,[5] strongly support this proposition. So far, most of the other S_N2 reactions reported have also involved anionic nucleophiles with neutral substrates.[6] Clearly, S_N1 reactions of neutral substrates cannot normally be studied by mass spectrometric techniques.

Previous studies of intermolecular S_N2 reactions between a neutral nucleophile and a cationic substrate are quite limited. A gas phase nucleophilic substitution on an allylic substrate bearing a leaving group (oxygen-protonated but-1-en-3-ol and *trans*-but-2-en-1-ol) with methanol[7a] was believed to proceed *via* the concerted S_N2' mechanism in competition with the classical S_N2 mechanism. The attack of glycine on a dimethylchloronium cation was shown by mass spectrometry[7b,c] to result in methyl cation transfer, but no direct evidence was presented for an S_N2 pathway. Some S_N2 methyl transfer was considered to occur for the diethylmethyloxonium ion with amine nucleophiles.[7d] Several studies on the fragmentation behavior of bifunctional compounds[8] have reported enhanced fragmentation peaks from the loss of small neutral molecules (*e.g.* NH_3,

‡ Permanent address: Department of Chemistry, A Mickiewicz University, 60780 Poznañ, Poland.

H_2O)[8b–i] which was postulated to have involved intramolecular S_N2 fragmentation.[8a] However, no detailed study on appearance potential energies has been reported for any of these systems.

Some years ago our research groups reported on the collisionally activated dissociation (CAD) of *N*-alkylpyridinium cations in the gas phase.[9] We demonstrated processes ($Py^+–R \rightarrow Py \cdots R^+ \rightarrow$products) of two main types: (*i*) to give products Py and R^+ in which rearrangement of the carbocation R^+ frequently occurred within the intermediate ion–molecule complex and (*ii*) to give products PyH^+ and the olefin formed by proton abstraction from R^+ in the ion–molecule complex. We now wish to report the extension of this work to an investigation of S_N2 processes.

Results and discussion

Our general strategy was to study gas phase S_N2 reactions which involve the reaction of neutral nucleophiles and cationic substrates containing neutral leaving groups. Considerable effort has been directed towards generating the S_N2 reactions *via* both intramolecular and intermolecular pathways.

Mass spectrometry techniques

In this work, we utilize Fourier transform ion cyclotron resonance mass spectrometry (FTICRMS) to study substitution reactions between cationic pyridinium substrates and neutral nucleophiles. However, while laser desorption ionization was used in the earlier studies involving reactions of *N*-benzylpyridinium and pyridine, electrospray ionization (ESI) has since been used in other studies to introduce the cationic substrates. ESI is a 'softer' ionization technique than laser desorption and has proven to be an excellent method for introducing intact pyridinium ions into the gas phase.[10]

Ion–molecule reactions in the *N*-benzylpyridinium–pyridine system

This study was initiated with the expectation that a benzyl ion would be transferred in bimolecular reactions from *N*-benzylpyridinium **1a** (Py^+Bz) and *N*-benzyl-4-dimethylaminopyridinium **1b** (4-Me_2NPy^+Bz) cations to various neutrals such as pyridine (Py), 4-ethylpyridine (4-EtPy), 4-dimethylaminopyridine (4-Me_2NPy) and quinoline (Q). Laser desorption of $Py^+Bz{\cdot}ClO_4^-$ and 4-$Me_2NPy^+Bz{\cdot}ClO_4^-$ resulted in intact molecular ions Py^+Bz (**1a**) and 4-Me_2NPy^+Bz (**1b**) at $m/z = 170$ and 213, respectively, and also in a fragment ion at $m/z = 91$, *i.e.* benzyl cation **2** (or tropylium) (Scheme 1, schemes describing

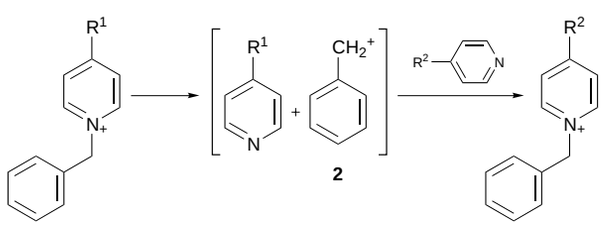

1a R^1 = H
b R^1 = 4-Me_2N

3a R^2 = H
b R^2 = Et
c R^2= 4-Me_2N

Scheme 1

gas phase reactions do not show the anion). No ions resulting from fragmentation of the pyridine ring were observed.

We formed the *N*-benzylpyridinium cations by laser desorption, as described in the Experimental section, and admitted either Py, 4-EtPy, 4-Me_2NPy or Q directly into the analyzer region using a precision leak valve until the pressure reached a value of 3×10^{-6} Torr (argon + neutral gas pressure). An example of ion intensities observed as a function of time after the ion formation laser pulse, when 4-EtPy was the neutral

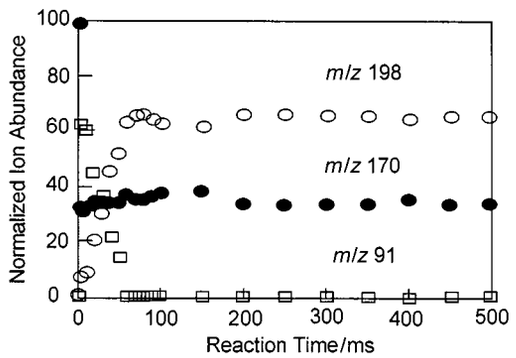

Fig. 1 Plot of the normalized ion abundance *vs.* the reaction time for the reaction of Py^+Bz (**1a**) (*m*/*z* 170) and 4-EtPy to form benzyl ion (**2**) (*m*/*z* 91) and 4-$EtPy^+Bz$ (**3b**) (*m*/*z* 198)

reactant, is given in Fig. 1. The kinetic behavior seen there is consistent with very rapid dissociation of the Py^+Bz ($m/z = 170$) to form benzyl ion **2** ($m/z = 91$), followed by somewhat slower addition of the benzyl cations to 4-EtPy to form 4-$EtPy^+Bz$ (**3b**, $m/z = 198$).

When benzyl ions were continually ejected from the analyzer cell during the reaction period, no products were observed. Attempts to induce a bimolecular benzyl-transfer reaction by adding kinetic energy to reactant Py^+Bz resulted in product ion formation. However, ejection of $m/z = 91$ benzyl ions during this reaction process again resulted in no product formation. Thus, we conclude that 'heating' the parent ions by adding kinetic energy only served to further fragment them *via* the CAD process, forming benzyl ions, which then reacted as previously documented[11] to form product ions. (When parent Py^+Bz was completely ejected from the analyzer cell immediately following laser desorption/ionization, no reaction was observed.)

Thus, no direct bimolecular reactions were observed between Py^+Bz (**1a**) and 4-Me_2NPy^+Bz (**1b**) cations and Py, 4-EtPy and Q neutrals (Scheme 1). Evidently in each case, unimolecular fragmentation of the parent cation gave benzyl cation **2** ($m/z = 91$), which then added to the neutrals to give Py^+Bz **3a** ($m/z = 170$), 4-$EtPy^+Bz$ **3b** ($m/z = 198$), 4-Me_2NPy^+Bz **3c** ($m/z = 213$) and Q^+Bz ($m/z = 220$) cations. Transfer of benzyl cation from Py^+Bz to 4-Me_2NPy should be exothermic ($\Delta H = -16$ kcal mol^{-1}, the heats of dissociation, $\Delta\Delta_f H$, of the Py^+Bz[9a] and 4-Me_2NPy^+Bz[12] are 41 and 57 kcal mol^{-1}, respectively), since 4-Me_2NPy is more basic than Py. These results suggest the presence of a barrier to ion–molecule reactions between 4-Me_2NPy^+Bz and Py, 4-EtPy and Q.

Intramolecular S_N2 reactions

N-Substituted pyridinium salts have been shown to be useful synthetic intermediates,[13] in addition to their applications in mechanistic studies of nucleophilic substitution reactions at sp^3-hybridized carbon.[1,3] Previous work in our groups has also demonstrated that these pyridinium compounds can be examined very effectively using FTICR mass spectrometry.[9,14] We selected a series of *N*-[ω-amino-(or ω-hydroxy-)alkyl]-pyridinium salts as substrates for the investigation of intramolecular S_N2 reactions.

Reactions of *N*-[ω-amino-(or ω-hydroxy-)alkyl]pyridinium salts in the solution phase have been reported:[15] pyridinium compounds derived from amino alcohols cyclize to form ethers (Scheme 2) or rearrange to aldehydes upon heating. Particularly interesting results came from the pyridinium salt **5** made from 5-aminopentanol. It was found to cyclize to give tetrahydropyran **6** *via* intramolecular nucleophilic attack by the oxygen. Moreover, derivatives **9** of *N*-(ω-aminoalkyl)pyridinium salts **8** are known to cyclize on heating to give heterocyclic compounds **10**. These results encouraged us to reinvestigate these reactions in the gas phase, with the intent of generating an intramolecular S_N2 reaction.

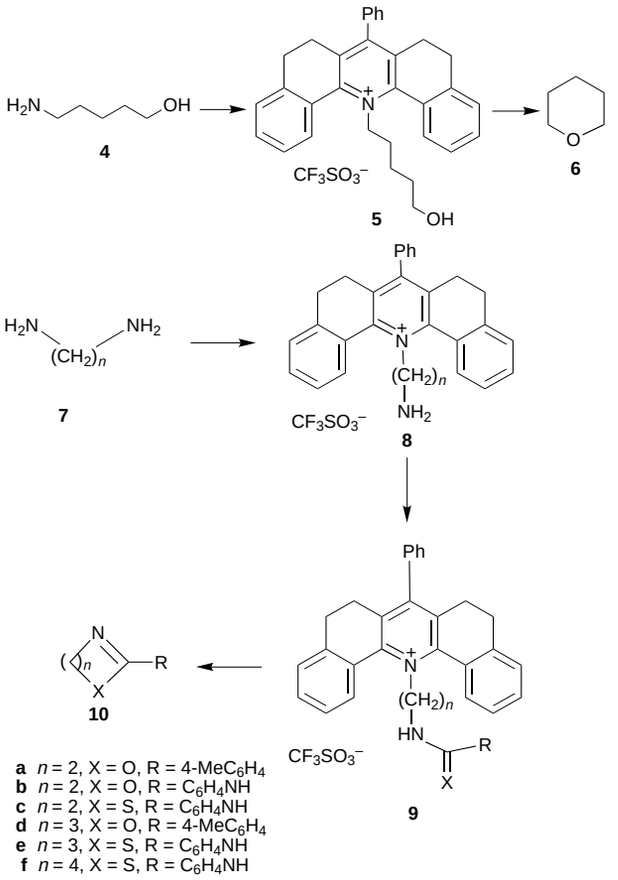

Scheme 2

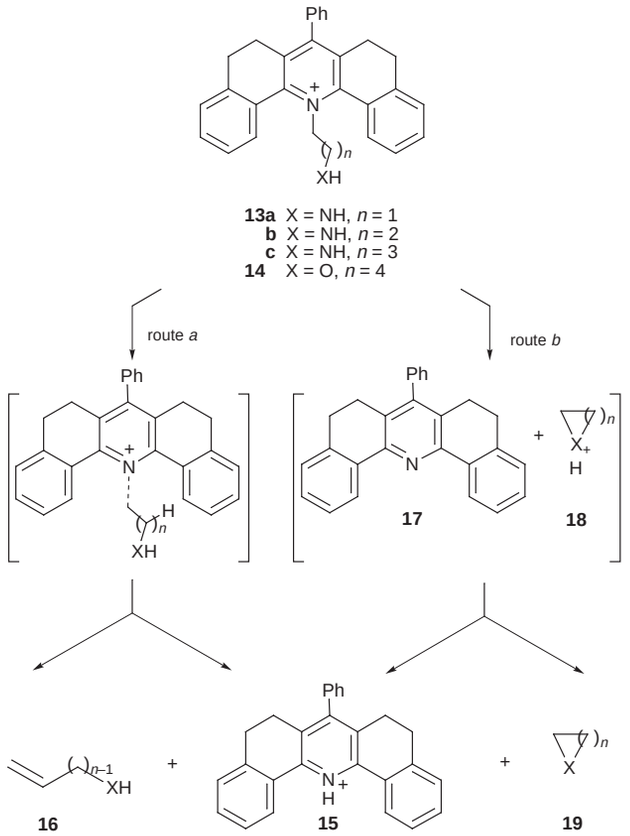

Scheme 3

Fragmentation pathways. Two distinct fragmentation pathways were observed in preliminary studies. The first is observed for **11a** and **11b**, it involves scission of the bond between the pyridinium substituted carbon and the pyridinium nitrogen producing a charged heterocyclic compound **12** and, presumably, a neutral substituted pyridine, which could not be detected by mass spectral means [reaction (3)]. The second is observed

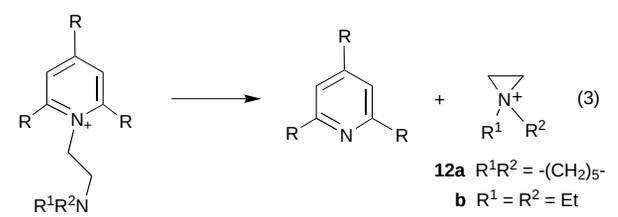

for **13a**–**c** and **14**, it also involves a similar C–N bond scission, but produces a protonated pyridinium cation **15** and another neutral product (Scheme 3).

When *N*-(2-piperidinoethyl)-2,4,6-triphenylpyridinium cation (**11a**) was trapped in the FTICR analyzer cell, two types of ion were detected after a delay period: the parent ion **11a** ($m/z = 419$) and product ion at $m/z = 112$, formed from the fragmentation of non-thermalized ion **11a** over several seconds in 10% yield [reaction (3)]. The structure of the product ion ($m/z = 112$) is assumed to be cyclic compound **12a**, which is thermodynamically the most stable product. When the isolated precusor ion was energized translationally *via* CAD by 5 kcal mol^{-1} over 10 μs, the reaction proceeded 100% to the product ion (**12a**). We estimate the internal energy of the unenergized parent ions to be approximately 23 kcal mol^{-1} (1.0 eV) based on the previously reported results.[9b] Similarly, when the CAD experiment was performed on *N*-[2-(diethylamino)ethyl]-2,4,6-trimethylpyridinium cation **11b**, the fragmentation of the parent cation **11b** was observed to give cation **12b** at $m/z = 100$. Again, the appearance potential energy was unmeasurably low. It is very clear that products $m/z = 112$ and 100, assumed to be the three-membered ring charged heterocycles (**12a**,**b**), are produced from intramolecular nucleophilic displacements of the neutral nitrogen on the side-chain α-carbon atom, *i.e.* compounds **11a**,**b** undergo intramolecular S_N2 reactions in the gas phase.

The three *N*-(ω-aminoalkyl)-5,6,8,9-tetrahydro-7-phenyldibenzo[*c*,*h*]acridinium salts **13a**–**c**, and *N*-(5-hydroxypentyl)-5,6,8,9-tetrahydro-7-phenyldibenzo[*c*,*h*]acridinium salt **14** were each subjected to the same experimental conditions as used for **11a**–**c**. In each case, only the protonated acridinium cation **15** ($m/z = 360$) and remaining unreacted parent ion were detected in the analyzer cell, as in Scheme 3. Cation **15** could be formed by two different routes. The first involves the dissociation of *N*-alkylacridinium cations to acridinium cation and olefins as reported in our previous work (Scheme 3, route *a*).[9b] Another path, considered more probable under the present conditions, involves an intramolecular nucleophilic attack of the exocyclic N or O atom on the side-chain α-carbon atom affording an ion-molecule pair of the corresponding cation **18** and acridine **17** (Scheme 3, route *b*), followed by fast proton transfer from cation **18** to substituted acridine to form the protonated acridinium cation **15**. No signal due to the cation **18** could be detected in our experiments; ion–molecule pair (**17**·**18**) has the same m/z as the corresponding **13** or **14** and it is reasonable to assume that transfer of the proton in **17**·**18** to give **15** and **19** is faster than dissociation of **17**·**18**. *N*-(ω-Aminoalkyl)-2,4,6-triphenylpyridinium salts **20a**,**b** as starting materials behaved similarly giving **21** and **19** [reaction (4)]. Attempts to measure the exact appearance potential energies for these reactions were unsuccessful as the required activation energy is quite low: their appearance potential energies were estimated in all these cases to be less than 23 kcal mol^{-1}.

We failed to prepare *N*-[4-(dialkylamino)butyl]-2,4,6-triphenylpyridinium tetrafluoroborate (**23**), which was expected to

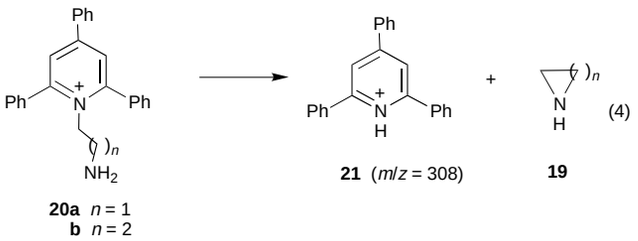

undergo S_N2 intramolecular reactions in the gas phase analogous to those of compounds **11a**,**b**. Reactions of triphenylpyrylium salt (**22**) and *N*,*N*-dialkylbutane-1,4-diamines in CH_2Cl_2 gave only 2,4,6-triphenylpyridine and dialkylpyrrolidinium salts **24**, evidently formed from spontaneous intramolecular S_N2 reactions in the solution phase *via* the expected pyridinium salts **23** (Scheme 4).

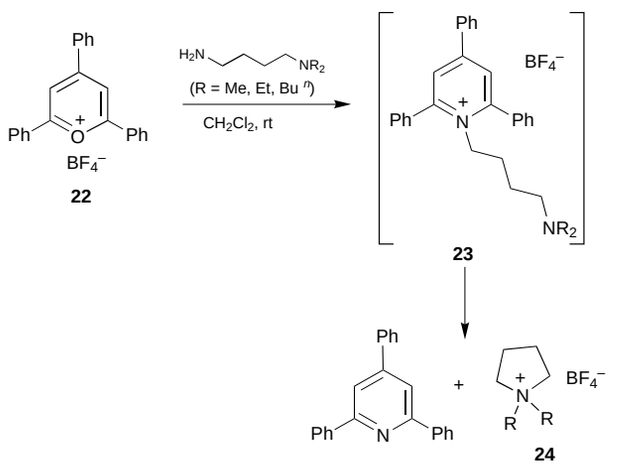

Scheme 4 (Solution phase)

In the gas phase, *N*-[3-(dimethylamino)propyl]-2,4,6-triphenylpyridinium cation (**25**) showed a different fragmentation pathway (Scheme 5). After the parent ion at *m*/*z* = 393 was isol-

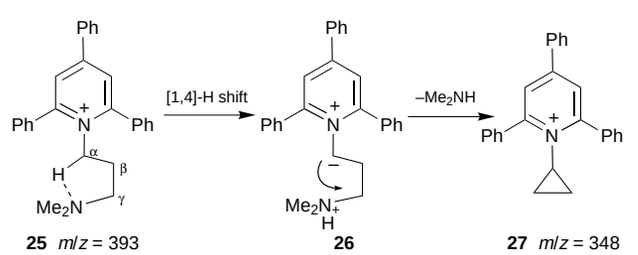

Scheme 5

ated and energized, a daughter ion at *m*/*z* = 348 was observed as the only product. We propose *N*-cyclopropyl-2,4,6-triphenylpyridinium cation (**27**) as the structure of this product, formed as shown in Scheme 5. Because of the unfavorable four-membered transition state for intramolecular S_N2 attack, the α-proton of the pyridinium ion was transferred to the ω-amino group *via* a [1,4] proton shift process with a five-membered transition state. Then, the newly formed carbanion center in **26** attacked the γ-carbon, which is now attached to a protonated dimethylammonium as the leaving group. The whole process produced the *N*-cyclopropylpyridinium cation **27** with *m*/*z* = 348.

Control experiments. The deuteroxy analog **28** of salt **14** was studied under the experimental conditions described above to ascertain the source of the proton transferred in the aforementioned acridinium reaction (Scheme 6). If the reaction pathway followed route *a*, a proton should be transferred from the β-CH_2 group to give **15**,[9b] but if the reaction proceeds *via*

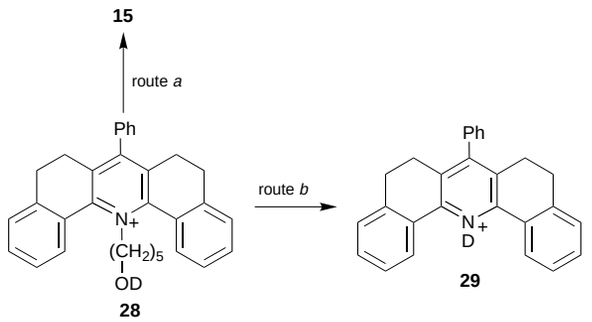

Scheme 6

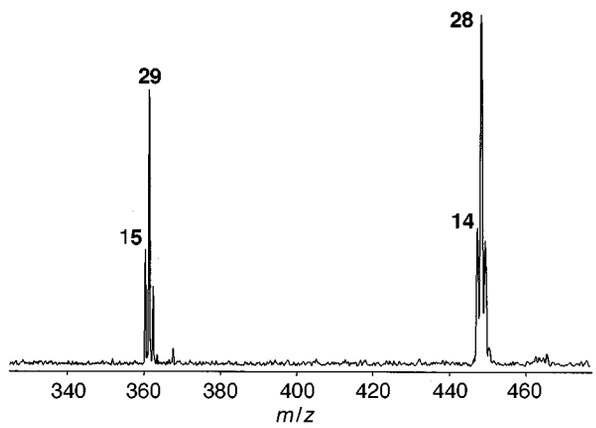

Fig. 2 ESI spectrum showing the control experiments for identifying the source of the proton transfer, **28**: deuteroxy analog of salt **14**; **29**: deuterated product ion; **14**, **15**: protic impurities

route *b*, a deuteron should be transferred from the deuteroxy group of the starting acridinium salt **28** to give **29**. The parent ion **28** (containing 27% protic impurity) was allowed to react in the analyzer cell during a 1 second delay. Following detection, it was observed that the reaction afforded product **29** with a 40% yield (Fig. 2). The slight increase in protic impurity in going from reactant to product (6% increase) was probably due to deuterium scrambling. The product forms from non-thermalized ions since no translational heating *via* radio-frequency (RF) excitation was used to drive the reaction. No further product formation was detected when longer reaction delays were used.

The second control experiment was designed to demonstrate the significantly different appearance potential energy that would be expected if the reaction had proceeded by route *a* in Scheme 3. *N*-Butyl-5,6,8,9-tetrahydro-7-phenyldibenzo[*c*,*h*]-acridinium salt **30** gave **15** as the sole fragment ion (*m*/*z* = 360) which can only arise by route *a* [reaction (5)] as no route *b* is

available. The appearance potential energy of **30** was measured to be 41.4 kcal mol^{-1} under the same CAD experimental conditions (Fig. 3, threshold fragmentation energy). This is very similar to the appearance potentials (38 to 62 kcal mol^{-1}) previously reported for *N*-alkyl substituted pyridinium salts (Table 1),[9b] but significantly different from those of ω-amino- or hydroxyalkyl substituted pyridinium or acridinium salts. This result supports the conclusion that the pyridinium and acridinium salts **13a**–**c**, **14**, **20a**,**b** in the gas phase undergo intramolecular (S_N2) nucleophilic substitution reactions as shown in reaction (3) and route *b* of Scheme 3.

Further attempted gas phase bimolecular S_N2 reactions of neutral nucleophiles with cationic substrates. Various *N*-methyl cations **32**–**35** introduced into the gas phase *via* electrospray

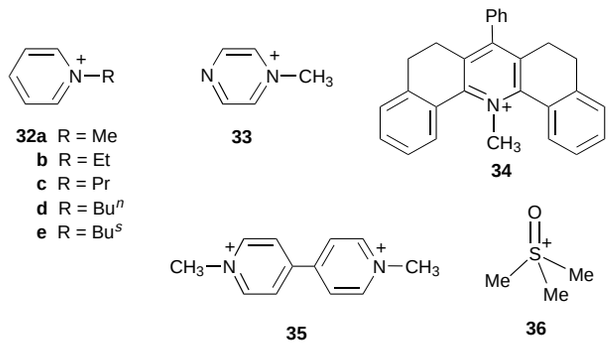

FTICR mass spectrometry were reacted with some neutral nucleophiles as summarized in Table 2. No evidence for gas phase S_N2 reactions was found for any of the systems studied. The 1-methylpyridinium cation (**32a**) undergoes proton transfer with several nucleophiles. With 4-dimethylaminopyridine (DMAP) **32a** forms the ion at $m/z = 200$, probably *via* loss of methane from *N*-(4-picolinyl)-4-dimethylaminopyridinium cation.

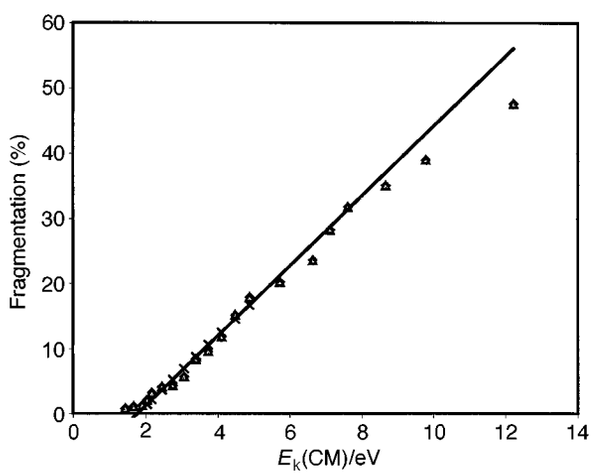

Fig. 3 Plot of the kinetic energy center-of-mass *vs.* the percent fragmentation for the dissociation reaction of pyridinium cation **30**

Table 1 Threshold energies (kcal mol^{-1}) for fragmentation for 1-substituted pyridinium cations (**30** and **32b**–**e**) to protonated pyridine and olefin

Compounds	**30**	**32b**	**32c**	**32d**	**32e**
Appearance energy of **15** or Py^+H	41.4	62[a]	47[a]	45[a]	38[a]

[a] Results from ref. 9*b*.

In the presence of 1-methylimidazole and tetramethylthiourea, no S_N2 reactions were observed for 1-methylpyrazinium cation (**33**). *N*-Methyl-5,6,8,9-tetrahydro-7-phenyldibenzo-[*c*,*h*]acridinium cation (**34**) is known to undergo S_N2 chemistry in solution;[3b] however, no S_N2 reactions were observed in the gas phase for **34** when DMAP, 1-methylimidazole, tetramethylthiourea or triphenylphosphine were used as the nucleophiles. Furthermore, only proton transfer and no S_N2 reactions were observed for the dimethylviologen dication (**35**) when DMAP and 1-methylimidazole were used as nucleophiles.

An ion–dipole complex at $m/z = 225$ was observed in high yield in the reaction between trimethylsulfoxonium cation (**36**) with tetramethylthiourea (Fig. 4), which demonstrates some interaction between the nucleophile and the substrate. Unfortunately, the ion–dipole complex could not be driven to the substitution products using RF excitation. The presence of a barrier on the potential energy surface probably prevents the S_N2 reaction and any excitation simply results in the conversion of complex back to reactants.

Theoretical study

The theoretical study of different S_N2 reactions has been of substantial interest for many years. Recent reviews by Shaik *et al.*[16a] and Minkin *et al.*[16b] give an overview of the methods used and also of the work done to elucidate the reaction mechanisms. Despite the many studies of the mechanism of S_N2 reactions, they continue to be an area of extensive current interest.[17]

The object of study. The theoretical investigation of intramolecular S_N2 reactions in the gas phase was performed on the basis of experimentally observed intramolecular nucleophilic substitution of the *N*-(ω-aminopropyl)-2,4,6-triphenylpyridinium cation (**20b**). Due to the size of that molecule, the three phenyl substituents in the pyridine ring were excluded and therefore, *N*-(ω-aminopropyl)pyridinium cation [**37**, reaction (6)] was studied as a model compound for the intramolecular S_N2 reaction. The intramolecular reaction was compared with the analogous intermolecular S_N2 reaction between the *N*-

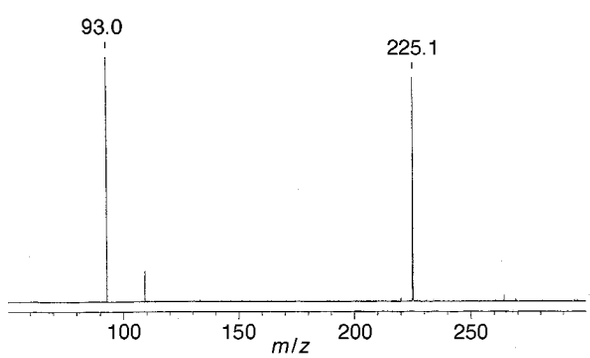

Fig. 4 ESI spectrum showing the complex **36**–$Me_2NC(S)NMe_2$ ($m/z = 225$) formed from the reaction between trimethylsulfoxonium cation **36** (m/z 93) and tetramethylthiourea

Table 2 Attempted intermolecular reactions in the gas phase using FTICRMS

Substrate/Nucleophile	*N*,*N*-Dimethyl aminopyridine	1-Methyl imidazole	Tetramethyl thiourea	Piperidine	Triphenyl phosphine
32a (m/z 94)	Nucleophilic aromatic substitution (m/z 123, 200)	Protonation of nucleophile (m/z 83)	Protonation of nucleophile (m/z 133)	—	No reaction
33 (m/z 95)	—	No reaction	No reaction	—	—
34 (m/z 374)	No reaction	No reaction	No reaction	—	—
35 (m/z 93, $z = 2$)	Protonation of nucleophile (m/z 123, 185)	Protonation of nucleophile (m/z 83)	—	—	—
36 (m/z 93)			Ion-induced dipole complex (m/z 225)	—	—

Table 3 AM1, PM3 and *ab initio* SCF calculated energies and the AM1 and PM3 calculated Gibbs activation free energies for the intra- (IA) and inter-molecular (IE) nucleophilic substitution reactions [reactions (6) and (7)]

	Intramolecular reaction						Intermolecular reaction					
	Reactants	TS	Products	E_a [a]	ΔE [b]	$\Delta G^{\ddagger}_{(IA)}$ [c]	Reactants	TS	Products	E_a [a]	ΔE [b]	$\Delta G^{\ddagger}_{(IE)}$ [c]
$\Delta_f H$(AM1) (kcal mol^{-1})	173.0	222.6	188.1	49.7	15.1	49.0	157.2	199.0	148.0	41.8	−9.2	46.5
$\Delta_f H$ (PM3)(kcal mol^{-1})	176.2	215.4	177.9	39.3	1.7	39.8	156.7	201.1	150.0	44.5	−6.7	47.5
HF/3-21G (Hartree) [d]	−416.8829	−416.8310	−416.8691	32.6	8.6	—	−418.0609	−418.0059	−418.0676	34.5	−4.2	—
MP2/3-21G [e] (Hartree) [d]	−417.7914	−417.7476	−417.7836	27.4	4.8	—	−418.9820	−418.9332	−418.9934	30.6	−7.1	—

[a] $E_a = \Delta_f H$(TS) − $\Delta_f H$(Reactant) in kcal mol^{-1}. [b] $\Delta E = \Delta_f H$(Product) − $\Delta_f H$(Reactant) in kcal mol^{-1}. [c] Calculated with eqns. (9) and (10), in kcal mol^{-1}. [d] 1 Hartree = 627.5 kcal mol^{-1}. [e] Single point MP2/3-21G*//HF/3-21G* calculation.

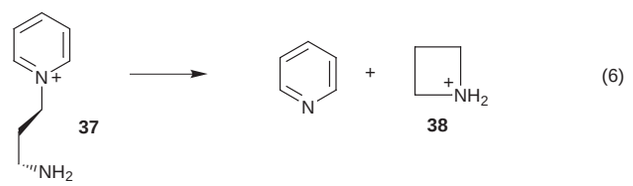

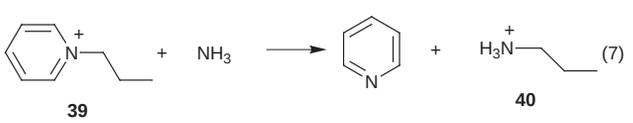

propylpyridinium cation (**39**) and free ammonia [reaction (7)]. The results of semiempirical AM1 and PM3 calculations suggested that ammonia is an adequate model compound for the description of the intermolecular S_N2 reaction. These results indicated that CH_3NH_2, a primary amine, as base has only a slightly higher value of the activation energy and reaction energy than does ammonia (2–3 kcal mol^{-1} calculated from AM1 and 2–5 kcal mol^{-1} calculated from PM3).

Computational method. Due to the size of the system, the quantum chemical semiempirical approach implemented in the MOPAC 6.0[18] program package was chosen for this study. The stationary points on the potential energy surfaces were calculated without applying any geometry constraints and using both AM1[19] and PM3[20] semiempirical parametrizations. The starting geometries of the reactants were defined proceeding from standard bond lengths and angles. Approximate transition state geometries were found by a grid scan of the potential energy surface and/or using the saddle point search method. The final geometries were optimized using the eigenvector following algorithm.[21] A gradient norm less than 0.01 kcal Å^{-1} was requested for all geometrical parameters in all calculations. The vibrational frequencies were calculated for all stationary points to verify the existence of minima and of true transition states (corresponding to a single negative eigenvalue of the Hessian). Finally, the intrinsic reaction coordinate method was employed to verify the existence of only one transition state between the two minima, corresponding to the reactant complex and the product complex of the reaction, respectively. This search started from the transition state and proceeded towards each of the minima. *Ab initio* calculations were also performed using the GAUSSIAN94[22] program package up to the MP2/3-21G*//HF/3-21G* level of theory.

Potential energy surfaces. The semiempirical calculations using AM1 and PM3 parametrizations lead to substantially different results. Whereas the calculated heats of formation (Table 3) of the stationary points for the intermolecular reaction were found to be very similar, with the PM3 activation energy 2.6 kcal mol^{-1} higher than the AM1 activation energy, the PM3 calculated heat of formation of the transition state for the intramolecular reaction was found to be substantially lower (7.2 kcal mol^{-1}) than that calculated using the AM1 parametrization (Table 3). Accordingly, the PM3 calculated activation energy of the intramolecular reaction is lower by 10.4 kcal mol^{-1} as compared to the AM1 result. As a result of this difference, the AM1 parametrization gives a higher activation energy (by about 7.8 kcal mol^{-1}) for the intramolecular reaction than that for the bimolecular S_N2 reaction, while the PM3 method predicts lower activation energy (by about 5.2 kcal mol^{-1}) for the intramolecular reaction.

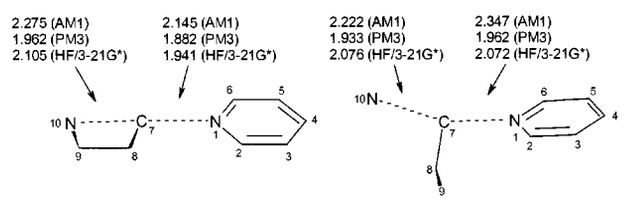

Fig. 5 Geometries of the transition state for the intra- and intermolecular reactions with bond lengths for N1–C7 and N10–C7 bonds in Å

The geometries of transition states (Table 4 and Fig. 5) calculated with semiempirical and *ab initio* methods are quite similar. The main difference in AM1 and PM3 geometries can be detected in the distances between the atoms along the chosen reaction coordinate (C7–N1 and N10–C7 in Table 4). The distances obtained from AM1 are overestimated, whereas the *ab initio* distances between the atoms along the reaction coordinate are between AM1 and PM3 results.

It is well known that semiempirical parametrizations overestimate the activation energies of intramolecular reactions[23] and, therefore, a direct comparison with the results for the intermolecular reactions is not fully justified. However, the semiempirical techniques usually give comparable trends of the activation barriers for a series of similar reactions. Calculations at the *ab initio* level of quantum theory are expected to give estimates of activation energies closer to the experimental data. Already small basis set *ab initio* SCF calculations (HF/3-21G) give significantly lower activation energy (32.6 kcal mol^{-1}) for the intramolecular reaction (Table 3) than the respective semiempirical treatments. The PM3 calculated activation energy is closer to the *ab initio* energy, but still substantially higher than the latter. The single point calculations using second order Møller–Plesset perturbation theory (MP2) further decrease the activation energy (to 27.4 kcal mol^{-1}). Both the Hartree–Fock and MP2 calculated activation energies for the intermolecular reaction are higher than the calculated activation energies for the respective intramolecular reaction (Table 3). The MP2 activation energy is already close to the experimentally proposed appearance energy estimated to be less than 23 kcal mol^{-1}. An application of more extended basis sets and higher level of theory is expected to further reduce the activation energy.[24] Such calculations on these systems would be expensive and unlikely to change our conclusions.

The results of the semiempirical quantum mechanical calcu-

Table 4 AM1, PM3 and *ab initio* calculated bond lengths (Å), bond angles (degrees), dihedral angles (degrees) and negative frequency for the transition states of the intra- (IA) and inter-molecular (IE) reactions (see Fig. 5 for the numbering)

	Intramolecular			Intermolecular		
	AM1	PM3	HF/3-21G*	AM1	PM3	HF/3-21G*
N1–C2	1.349	1.364	1.334	1.349	1.364	1.334
C2–C3	1.405	1.392	1.378	1.406	1.393	1.379
C3–C4	1.398	1.394	1.385	1.397	1.393	1.384
C4–C5	1.397	1.393	1.385	1.398	1.394	1.385
C5–C6	1.406	1.393	1.378	1.405	1.392	1.378
C6–N1	1.349	1.363	1.334	1.349	1.365	1.335
C7–N1	2.275	1.962	2.105	2.222	1.933	2.076
C7–N1–C2	121.09	119.94	120.18	120.39	120.53	119.88
C7–N1–C2–C3	177.66	177.47	177.92	177.99	178.13	176.44
C8–C7	1.493	1.530	1.537	1.465	1.508	1.523
C8–C7–N1	96.47	96.80	94.43	100.98	99.73	96.86
C8–C7–N1–C2	71.43	81.82	90.83	116.26	92.61	108.51
C9–C8	1.543	1.527	1.544	1.509	1.514	1.538
C9–C8–C7	101.14	98.15	97.62	113.78	112.84	112.31
C9–C8–C7–N1	180.45	180.52	174.65	93.15	91.68	87.12
N10–C7	2.145	1.882	1.941	2.347	1.962	2.072
N10–C7–N1	174.39	177.65	175.89	161.56	161.65	166.12
N10–C7–N1–C2	69.23	71.09	85.92	58.33	84.20	63.37
ν/cm^{-1}	−544.09	−719.18	−549.82	−405.09	−738.38	−542.60

Table 5 AM1 SCF calculated dependence of the activation energy on the number of the carbon atoms in the alkyl chain of *N*-aminoalkylpyridinium cations [see also reactions (6) and (7)]

n	E_a [a]/kcal mol[1]	ΔE [b]/kcal mol^{-1}
2	49.7	15.1
3	40.6	−5.3
4	38.7	−12.9

[a] $E_a = \Delta_f H$(TS) − $\Delta_f H$(Reactant). [b] $\Delta E = \Delta_f H$(Product) − $\Delta_f H$(Reactant).

lations indicate the dependence of the activation energy of reaction on the size of the alkyl chain in the *N*-(aminoalkyl)-pyridinium cation. The compounds with a longer alkyl chain are predicted to have lower activation energies of reaction (Table 5). According to our calculations, the addition of the phenyl substituents to the pyridine ring (**20b**) increases the semiempirically calculated activation energy by approximately 2 kcal mol^{-1}. We also note increasing stability of the products over the reactants, which is a consequence of less ring strain in **38**.

The experimentally observed differences in the intramolecular and intermolecular nucleophilic reactivity of compounds can also be caused by probabilistic factors. In the case of the intermolecular reaction between the *N*-alkylpyridinium cation and ammonia [reaction (7)], the reactants must collide to form the reactive complex. This process is of comparatively low probability in the gas phase at low pressure. In the case of the *N*-(ω-aminopropyl)pyridinium cation [**37**, reaction (6)], the reactive amino group is directly connected to the C9 carbon atom of the propyl group and, therefore, it is always near the reaction center (C7). The rotational barrier of the amino group around the C8–C9 bond is very low (1–2 kcal mol^{-1}) and thus the nitrogen (N10) lone pair can easily approach the C7 atom of the propyl group.

Gibbs activation free energy. Transition state theory (TST)[25] can be applied to calculate the Gibbs activation free energy for the reactions considered in the present study. According to the TST, the rate constant of a chemical reaction is defined by eqn. (8),[25] where χ is the transmission coefficient (usually

$$k_r = \chi \frac{k_B T}{h} \frac{Q^{\ddagger}}{\Pi_i Q_i^R} e^{-E_a/RT} \quad (8)$$

close to 1), k_B is the Boltzmann constant, h is Planck's constant, T is temperature (in K), $Q^{\ddagger}$ is the partition function for the transition state, Q_i^R are the partition functions for the reactants R, and E_a is the activation energy of the reaction. The partition function for each species can be expressed as a product of the respective electronic (Q_{el}), translational (Q_{trans}), rotational (Q_{rot}) and vibrational (Q_{vib}) partition functions at a given temperature. Each of these components can be calculated by standard statistical mechanics methods.[25]

By combining the definition of the Gibbs activation free energy of the reaction, $\Delta G^{\ddagger} = -RT\ln K^{\ddagger}$ (R is the molar gas constant), and the TST expression for the rate constant (8), eqns. (9) and (10) are obtained for the activation free energy of

$$\Delta G_{IA}^{\ddagger} = E_a^{IA} - RT\ln\frac{Q^{\ddagger}}{Q_{IA}^{A}} \quad (9)$$

$$\Delta G_{IE}^{\ddagger} = E_a^{IE} - RT\ln\frac{Q^{\ddagger} N_A}{Q_{IE}^{A} Q_{IE}^{B}} \quad (10)$$

the intra- (IA) and inter-molecular (IE) S_N2 reaction, respectively.

The Gibbs activation free energies for the intra- and intermolecular nucleophilic substitution reactions [reactions (6) and (7)] using the AM1 and PM3 calculated activation energies and the respective partition functions (Table 6) are given in Table 3. In the case of PM3 parametrizations, the intramolecular nucleophilic substitution reaction is predicted to have lower activation free energy than the respective intermolecular S_N2 reaction. The AM1 calculated activation free energy shows the opposite direction and that is due to the deficiencies in the AM1 parametrization for the study of the intramolecular interaction.

Therefore, the results of our theoretical modelling (PM3 and *ab initio*) suggest that bimolecular S_N2 reactions involving positively charged substrates with neutral leaving groups are difficult to induce in the gas phase. Notably, all our attempts to observe such reactions in the gas phase have so far failed. However, the intramolecular nucleophilic displacement with the cyclic transition state has a much lower predicted activation free energy in the gas phase and, therefore, can be observed.

Conclusions

Bimolecular S_N2 reactions of positively charged substrates with neutral leaving groups are evidently difficult to induce in the gas phase and all our attempts have failed. However, we have succeeded in demonstrating intramolecular S_N2 displacement in which cyclic transition states lead to the formation of charged

Table 6 Different contributions to the calculated activation free energy ($RT\ln Q$ kcal mol^{-1}) of the intra- and inter-molecular nucleophilic substitution reaction [reactions (6) and (7)] at 300 K[a]

	$RT\ln Q_{vib}$	$RT\ln Q_{rot}$	$RT\ln Q_{trans}$	$RT\ln \Pi Q$
AM1: Intramolecular reaction (IA)				
TS (‡)	5.5	8.1	37.3	51.0
Reactant (A)	4.7	8.1	37.3	50.1
			$RT\ln (Q^{‡}_{IA}/Q^{A}_{IA}) = 0.9$	
AM1: Intermolecular reaction (IE)				
TS (‡)	7.5	8.2	37.3	53.1
Reactant (A)	3.3	7.8	57.2	48.3
Reactant (B)	3×10^{-3}	2.5	35.5	42.1
			$RT\ln [Q^{‡}_{IE}/(Q^{A}_{IE}Q^{B}_{IE})] = -37.3$	
PM3: Intramolecular reaction (IA)				
TS (‡)	4.3	8.1	37.3	49.7
Reactant (A)	4.8	8.1	37.3	50.2
			$RT\ln (Q^{‡}_{IA}/Q^{A}_{IA}) = -0.5$	
PM3: Intermolecular reaction (IE)				
TS (‡)	5.2	8.2	37.3	50.7
Reactant (A)	3.4	7.8	37.2	48.4
Reactant (B)	1×10^{-3}	2.5	35.5	38.0
			$RT\ln [Q^{‡}_{IE}/(Q^{A}_{IE}Q^{B}_{IE})] = -35.7$	

[a] Partition functions are obtained from semiempirical thermodynamic calculations at optimized single point geometries.

heterocycles. Quantum chemical treatment of these systems using both the PM3 semiempirical and *ab initio* models reflects a substantial preference for intramolecular as compared to intermolecular reactions.

Experimental

The preparation and characterization of most of the compounds used in this study has been published before by this group.[15,26] Other new pyridinium salts were made following literature methods.[15] *N*,*N*-Diethylbutane-1,4-diamine and *N*,*N*-dibutylbutane-1,4-diamine were prepared employing a reported method.[27]

N-(Dimethylaminopropyl)-2,4,6-triphenylpyridinium tetrafluoroborate (25)

A solution of *N*,*N*-dimethylpropane-1,3-diamine (1.5 mmol) and triethylamine (1.5 mmol) in CH_2Cl_2 (5 ml) was added to a solution of 2,4,6-triphenylpyrrylium tetrafluoroborate (1.5 mmol) in CH_2Cl_2 (15 ml) at room temp. The reaction mixture was stirred for 4 h, then 5 drops of AcOH were added and the resulting mixture was stirred overnight. After adding dry Et_2O (75 ml) to the yellow–red solution, pure yellow solid was obtained after filtration and drying in 86% yield, mp 190–192 °C; δ_H($CDCl_3$, 300 MHz) 7.70–7.85 (8 H, m), 7.55–7.65 (6 H, m), 7.43–7.54 (3 H, m), 4.42–4.50 (2 H, m), 1.60–1.75 (10 H, m); δ_C($CDCl_3$, 75 MHz) 156.4, 155.8, 134.1, 132.8, 131.9, 130.9, 129.6, 129.3, 129.0, 128.1, 126.8, 55.9, 53.6, 44.5, 27.4.

Laser desorption experiments

These experiments were performed in a Finnigan FTMS (formerly Nicolet) FTICR mass spectrometer equipped with an IonSpec data station utilizing a 3T superconducting magnet and a heated inlet system equipped with dual precision leak valves. The vacuum chamber was pumped by a 300 l s^{-1} oil diffusion pump maintaining the background pressure of the system below $1–2 \times 10^{-8}$ Torr when the solids probe was inserted into the vacuum chamber. Ions formed by laser desorption were trapped in a 1.0 cubic inch cell with a trap voltage of 2 V.

For laser desorption experiments, a quench pulse was applied to the trap plates to eject all ions from the cell. Next, a focused CO_2 laser pulse desorbed *N*-benzylpyridinium cations from a dried sample of *ca.* 1 mm thickness on a stainless steel solids probe tip. A Lumonics TE 860 pulsed carbon dioxide laser, operating in the static gas mode, was used to desorb the ions. The laser was focused through a 7.63 cm focal length, 1.27 cm diameter ZeSe lens onto the end of the solids probe tip. The area of laser irradiation was 0.8 mm^2. The laser was fired with an average energy of 1.0 J per pulse, as measured at the laser exit window. Ten laser pulses were fired at the solids probe tip in its initial position and then it was rotated manually to provide a fresh surface for the next set of pulses. The ions formed were stored in the FTICR analyzer cell for 750 ms or more in the presence of 5×10^{-7} Torr of argon and at least partially thermalized by ion/neutral collisions. Next, a series of ejection sweeps was applied to isolate the molecular ion of interest. Reagent gases were purified by multiple freeze–pump–thaw cycles and leaked into the chamber up to a pressure of $1–3 \times 10^{-6}$ Torr *via* a variable leak valve. Then a variable delay time allowed the ion–molecule reactions to take place. The ions were excited by the standard frequency chirp excitation method and 64 K time-domain points were acquired during broadband detection (20–400 amu). For each reaction delay time, 10 scans were averaged to enhance the signal to noise ratio.

Electrospray experiments

The experimental setup and the ESI source have been described in the preceding paper[28] and in detail previously.[29]

The samples were dissolved in a 50 : 50 water–methanol solution at a concentration of 0.1 mg ml^{-1} and were introduced into the ESI source at a flow rate of 1μl min^{-1}.

Collisionally activated dissociation

The experimental procedure CAD first utilized a 100 ms quench pulse to remove any ions remaining in the cell from a previous experiment. After the quench pulse, an ion accumulation period of 5000 μs duration followed. During the ion accumulation, the electrostatic optics were pulsed to allow accumulation of ions in the analyzer cell. The precursor pyridinium cation was isolated using swept-frequency ejection pulses of 200 ms duration to eject all other ions. Argon was introduced *via* a leak valve to a background pressure of 2×10^{-7} Torr. The precursor ions were excited using a variable amplitude on-resonance excitation pulse of 10 μs duration. A 6.5–19 V range of RF amplitudes was used to study the energy dependence of the CAD process. Following the excitation of the precursor ion, a 0.25 s delay was introduced to allow for collisions to occur resulting in fragmentation of the ion. Calculation of the threshold energies has been described elsewhere.[9a]

Deuterium labeling experiments

The hydroxy deuterated analog **28** of salt **14** was formed by dissolving 0.5 mg of salt **14** in 2.5 ml D_2O with stirring for 2 h. Following the deuterium transfer, the compound was immediately electrosprayed from this solution in order to minimize deuterium scrambling. Mass spectral analysis showed that 73% of the parent contained the deuterium label. The parent ion **28** was isolated using swept-frequency ejection pulses; however, to minimize inadvertent RF-heating of the labeled compound the protic impurity was not ejected prior to the reaction delay. A slight increase in the protic impurity of the product (33%) may be attributed either to deuterium scrambling during the reaction delay or to uneven RF excitation during the detection process.

Acknowledgements

We thank Dr Toomas Tamm for his help with some calculations. The electrospray FTICR instrumentation was purchased with a grant from the National Science Foundation Chemical Instrumentation Program.

References

1 A. R. Katritzky and B. E. Brycki, *Chem. Soc. Rev.*, 1990, **19**, 83.

2 C. K. Ingold, *Structure and Mechanism in Organic Chemistry*; (*a*) Cornell University Press, New York, 1st edn., 1953, pp. 306–418; (*b*) Cornell University Press, New York, 2nd edn., 1969, pp. 418–610.
3 (*a*) A. R. Katritzky and B. E. Brycki, *J. Phys. Org. Chem.*, 1988, **1**, 1; (*b*) A. R. Katritzky and K. Sakizadeh, *Heterocycles*, 1985, **23**, 1765; (*c*) A. R. Katritzky and G. Musumarra, *Chem. Soc. Rev.*, 1984, **13**, 47.
4 (*a*) W. N. Olmstead and J. I. Brauman, *J. Am. Chem. Soc.*, 1977, **99**, 4219; (*b*) C.-C. Han, J. A. Dodd and J. I. Brauman, *J. Phys. Chem.*, 1986, **90**, 471; (*c*) J. A. Dodd and J. I. Brauman, *J. Phys. Chem.*, 1986, **90**, 3559; (*d*) J. I. Brauman, *J. Mass Spectrom.*, 1995, **30**, 1649.
5 (*a*) S. T. Graul and M. T. Bowers, *J. Am. Chem. Soc.*, 1991, **113**, 9696; (*b*) D. M. Cyr, L. A. Posey, G. A. Bishea, C.-C. Han and M. A. Johnson, *J. Am. Chem. Soc.*, 1991, **113**, 9697; (*c*) J. L. Wilbur and J. I. Brauman, *J. Am. Chem. Soc.*, 1991, **113**, 9699.
6 (*a*) R. C. Lum and J. J. Grabowski, *J. Am. Chem. Soc.*, 1993, **115**, 7823; (*b*) A. A. Viggiano, R. A. Morris, T. Su, B. D. Wladkowski, S. L. Craig, M. Zhang and J. I. Brauman, *J. Am. Chem. Soc.*, 1994, **116**, 2213; (*c*) B. D. Wladkowski, J. L. Wilbur and J. I. Brauman, *J. Am. Chem. Soc.*, 1994, **116**, 2471; (*d*) C. Li, P. Ross, J. E. Szulejko and T. B. McMahon, *J. Am. Chem. Soc.*, 1996, **118**, 9360.
7 (*a*) E. Dezi, A. Lombardozzi, A. Pizzabiocca, G. Renzi and M. Speranza, *J. Chem. Soc., Chem. Commun.*, 1995, 547; (*b*) R. A. J. O'Hair, M. A. Freitas, S. Gronert, J. A. R. Schmidt and T. D. Williams, *J. Org. Chem.*, 1995, **60**, 1990; (*c*) R. A. J. O'Hair, M. A. Freitas and T. D. Williams, *J. Org. Chem.*, 1996, **61**, 2374; (*d*) G. Occhiucci, M. Speranza, L. J. de Koning and N. M. M. Nibbering, *J. Am. Chem. Soc.*, 1989, **111**, 7387.
8 (*a*) K. Sailer and M. Hesse, *Helv. Chim. Acta* , 1968, **51**, 1817; (*b*) J. K. Kim, M. C. Findlay, W. G. Henderson and M. C. Caserio, *J. Am. Chem. Soc.*, 1973, **95**, 2184; (*c*) F. V. Gaever, J. Monstrey and C. C. V. de Sande, *Org. Mass Spectrom.*, 1977, **12**, 200; (*d*) H. E. Audier, M. C. Perret, J. C. Tabet and P. Varenne, *Org. Mass Spectrom.*, 1978, **13**, 315; (*e*) R. J. Weinkam, *J. Chem. Org.*, 1978, **43**, 2581; (*f*) P. Longevialle, J.-P. Girard, J.-C. Rossi and M. Tichý, *Org. Mass Spectrom.*, 1979, **14**, 414; (*g*) D. V. Davis and R. G. Cooks, *Org. Mass Spectrom.*, 1981, **16**, 176; (*h*) V. H. Wysocki, D. J. Burinsky and R. G. Cooks, *J. Org. Chem.*, 1985, **50**, 1287; (*i*) M. L. Larrivee and J. Allison, *J. Am. Chem. Soc.*, 1990, **112**, 7134.
9 (*a*) A. R. Katritzky, C. H. Watson, Z. Dega-Szafran and J. R. Eyler, *J. Am. Chem. Soc.*, 1990, **112**, 2471; (*b*) A. R. Katritzky, C. H. Watson, Z. Dega-Szafran and J. R. Eyler, *J. Am. Chem. Soc.*, 1990, **112**, 2479.
10 A. R. Katritzky, P. A. Shipkova, R. D. Burton, S. M. Allin, C. H. Watson and J. R. Eyler, *J. Mass Spectrom.*, 1995, **30**, 1581.
11 A. R. Katritzky, Z. Dega-Szafran, R. Ramanathan and J. R. Eyler, *Org. Mass Spectrom.*, 1994, **29**, 96.
12 Calculated in the same way as for $Py^{+}Bz$ by AM1.
13 (*a*) For a review, see A. R. Katritzky, *Tetrahedron*, 1980, **36**, 679; (*b*) A. R. Katritzky and C. M. Marson, *Angew. Chem., Int. Ed. Engl.*, 1984, **23**, 420.
14 C. H. Watson, G. Baykut, Z. Mowafy, A. R. Katritzky and J. R. Eyler, *Anal. Instrum.*, 1988, **17**, 155.
15 (*a*) A. R. Katritzky, R. T. Langthorne, R. C. Patel and G. Lhommet, *Tetrahedron*, 1981, **37**, 2383; (*b*) intramolecular reactions of some neutral amines, including haloalkylamines, in solution phase have been reviewed: A. J. Kirby, *Adv. Phys. Org. Chem.*, ed. V. Gold and D. Bethell, 1980, **17**, 183.
16 (*a*) S. S. Shaik, H. B. Schlegel and S. Wolfe, *Theoretical Aspects of Physical Organic Chemistry: The SN2 Mechanism*, Wiley, New York, 1992; (*b*) V. I. Minkin, B. Y. Simkin and R. M. Minyaev, *Quantum Chemistry of Organic Compounds – Mechanism of Reactions*, Springer Verlag, Berlin, 1990.
17 (*a*) U. Maran, T. A. Pakkanen and M. Karelson, *J. Chem. Soc., Perkin Trans. 2*, 1994, 2445; (*b*) M. N. Glukhovtsev, A. Pross and L. Radom, *J. Am. Chem. Soc.*, 1995, **117**, 2024; (*c*) M. N. Glukhovtsev, A. Pross and L. Radom, *J. Am. Chem. Soc.*, 1996, **118**, 6273; (*d*) F. M. Bickelhaupt, E. J. Baerends and N. M. M. Nibbering, *Chem. Eur. J.*, 1996, **2**, 196.
18 J. J. P. Stewart, MOPAC Program Package, 1989 QCPE, No 455.
19 M. J. S. Dewar, E. G. Zoebisch, E. F. Healy and J. P. Stewart, *J. Am. Chem. Soc.*, 1985, **107**, 3902.
20 J. J. P. Stewart, *J. Comput. Chem.*, 1989, **10**, 209.
21 J. Baker, *J. Comput. Chem.*, 1986, **7**, 385.
22 M. J. Frisch, G. W. Trucks, H. B. Schlegel, P. M. W. Gill, B. G. Johnson, M. A. Robb, J. R. Cheeseman, T. A. Keith, G. A. Petersson, J. A. Montgomery, K. Raghavachari, M. A. Al-Laham, V. G. Zakrzewski, J. V. Ortiz, J. B. Foresman, J. Cioslowski, B. B. Stefanov, A. Nanayakkara, M. Challacombe, C. Y. Peng, P. Y. Ayala, W. Chen, M. W. Wong, J. L. Andres, E. S. Replogle, R. Gomperts, R. L. Martin, D. J. Fox, J. S. Binkley, D. J. Defrees, J. Baker, J. P. Stewart, M. Head-Gordon, C. Gonzalez and J. A. Pople, GAUSSIAN94, Revision B.1, Gaussian, Inc., Pittsburgh, PA, 1995.
23 (*a*) J. J. Dannenberg and R. Rios, *J. Phys. Chem.*, 1994, **98**, 6714; (*b*) U. Maran, M. Karelson and A. R. Katritzky, *Int. J. Quant. Chem., Quant. Biol. Symp. 23*, 1996, **60**, 41.
24 L. A. Curtiss, K. Raghavachari, G. W. Trucks and J. A. Pople, *J. Chem. Phys.*, 1991, **94**, 7221.
25 J. I. Steinfeld, J. S. Francisco and W. L. Hase, *Chemical Kinetics and Dynamics*, Prentice-Hall, New Jersey, 1989.
26 A. R. Katritzky, J. B. Bapat, R. M. Claramunt-Elguero, F. S. Yates, A. Dinculescu, A. T. Balaban and F. Chiraleu, *J. Chem. Res.* (*M*), 1978, 4783.
27 L. H. Amundsen and J. J. Sanderson, *Org. Synth.*, 1955, *Coll. Vol III*, 256.
28 A. R. Katritzky, R. D. Burton, P. A. Shipkova, M. Qi, C. H. Watson and J. R. Eyler, following paper.
29 A. R. Katritzky, P. A. Shipkova, M. Qi, D. A. Nichols, R. D. Burton, C. H. Watson, J. R. Eyler, T. Tamm, M. Karelson and M. C. Zerner, *J. Am. Chem. Soc.*, 1996, **118**, 11 905.

Paper 7/08462E
Received 24*th November* 1997
Accepted 19*th January* 1998